Materials Science in Semiconductor Processing 39 (2015) 416–425

Contents lists available at ScienceDirect

Materials Science in Semiconductor Processing

journal homepage: www.elsevier.com/locate/mssp

Review

Spray coating methods for polymer solar cells fabrication: A review

F. Aziz [a,b], A.F. Ismail [a,b,*]

[a] Advanced Membrane Technology Research Centre (AMTEC), Universiti Teknologi Malaysia (UTM), 81310 Johor Bahru, Johor, Malaysia
[b] Faculty of Petroleum and Renewable Energy Engineering, Universiti Teknologi Malaysia (UTM), 81310 Johor Bahru, Johor, Malaysia

ARTICLE INFO

Keywords:
Spray coating
Polymer solar cells
Blade coating
Printing methods

ABSTRACT

The main focus of this review article is the introduction of relevant parameters in spray coating processes to provide better understanding on controlling the morphology of spray coated thin films for producing high performance polymer solar cells (PSC). Three main parameters have been identified as major influences on the spray coating processes. These are nozzle to substrate distance, solvent and mixed solvents effects, and substrate temperature and annealing treatment. Such spray coating techniques show great potential for large scale production, since these methods have no limitation in substrate size and low utilization of polymers which is promising to substitute the conventional spin coating methods. Currently available printing and coating methods are also briefly discussed in this review.

Contents

Abbreviations: CN-ether-PPV, poly[oxa-1,4-phenylene-1,2-(1-cyano)-ethenylene-2,5-dioctyloxy-1,4-phenylene-1,2-(2-cyano)-ethenylene-1,4-phenylene]; M3EH-PPV, poly[2,5-dimethoxy-1,4-phenylene-1,2-ethenylene-2-methoxy-5-(2-ethylhexyloxy)-(1,4-phenylenevinylene-1,2-ethenylene)]; P3HT, poly (3-hexylthiophene 2,5-diyl); PCBM, phenyl-C_{61}-butyric acid methyl ester; P3MHOCT, poly-(3-(2-methylhexyloxycarbonyl)dithiophene); PCDTBT, poly[N-9′-hepta-decanyl-2,7-carbazole-alt-5,5-(4′,7′-di-2-thienyl-2′,1′,3′-benzothiadiazole)]; PFB, poly(9,9′-dioctylfluorene-co-bisN,N′-(4-butylphenyl)-bis-N,N′-phenyl-1,4-phenylenediamine); F8BT, poly(9,9′-dioctylfluorene-co-benzothiadiazole); PBDTTT-C-T, poly{[4,8-bis-(2-ethyl-hexyl-thiophene-5-yl)-benzo[1,2-b:4,5-b0]dithiophene-2,6-diyl]-alt-[2-(20-ethyl-hexanoyl)-thieno[3,4-b]thiophen-4,6-diyl]}; PEDOT:PSS, poly (3,4-ethylenedioxythiophene)–poly (styrenesulfonate)

* Corresponding author at: Advanced Membrane Technology Research Centre (AMTEC), Universiti Teknologi Malaysia (UTM), 81310 Johor Bahru, Johor, Malaysia. Tel.: +607 5535592; fax: +607 5535625.
E-mail address: afauzi@utm.my (A.F. Ismail).

http://dx.doi.org/10.1016/j.mssp.2015.05.019
1369-8001/

1. Introduction

One of the major issues in encouraging developments of polymer solar cells (PSC) commercialization is finding a roll-to-roll compatible, high yielding process for low cost production [1–4]. Blade coating [5,6], spin coating [7–9], spray coating [10–15], dip coating [1], screen printing [16], gravure printing [17], and ink-jet printing [18–20] are among the methods used to fabricate the PSC. Table 1 lists the previous researches on PSC prepared using different methods. Spin coating is a standard method that has been used to produce uniform coatings of desired thickness, however, high materials wastage of more than 90% for spin coating makes the materials costs to rise as the film-coated area becomes larger [5,21]. Ink-jet printing methods have attracted attention as part of a promising cost-efficient process for PSC fabrication due to its efficient materials usage, and its direct and precise patterning with a resolution of 20–30 μm, unlike that of spin coating and other conventional methods [22,23]. Unfortunately, ink-jet printing is not easily adaptable to mass volume manufacture, due to its low volume throughput and complexity [24].

Blade coating and slot-die coating are suited to high volume, scale up and commercialization of PSC, since these methods are compatible with high speed, high volume, and low cost roll-to-roll production. A power conversion efficiency (PCE) of more than 6% can be achieved in a blade coating process due to the ability of the donor and acceptor to quickly self-assemble into the desired ordered and interpenetrating morphology during the blade coating process in the absence of centrifugal force [5]. However, in blade coating methods, the wet film formation is relatively low compared to spin coating, and aggregate or crystallite formation at high concentration often occurs during blade coating [25]. Dip coating process is a commonly used method for conventional dyeing and can provide easy and fast deposition of polymer films over a large area [1]. The dip coating process is prompt with single pass formation of the film compared to other spray coating and inkjet print processes and the films formed are free-pinhole [1,26]. However, the formation of the dip coated film is a slow natural drying process making it incompatible for high volume production.

The spray coating techniques have a great potential for large scale production, since these methods have no-limitation in substrate size and low utilization of polymers, promising to substitute the conventional process which is spin coating methods [27]. The ability to access a broad spectrum of fluids with various rheologies, making the production of fully spray coated PSC devices, is possible. However, the usage of spray coating in the production of PSC is faced with one main issue, namely higher film thickness and roughness [28]. Thus, most of the current research concerns on optimizing the morphology of an active layer by using high boiling point solvents [29], additives, solvents mixtures, postthermal annealing [28,29], and additional spray coating methods [11]. To the best of our knowledge, a limited number of review articles have been published on the processing methods of PSC specifically spray coating methods. Therefore, this review aims to summarize relevant parameters in spray coating processes to provide better understanding on controlling the morphology of the spray coated thin films in producing a high performance PSC and commercialization of this technology.

Table 1
List of previous researches on PSC prepared using different methods.

Active layer	Methods	References	Year
M3EH-PPV:CN-ether-PPV	Spin coating	[30]	2005
P3HT:PCBM	Blade coating	[6]	2009
P3MHOCT:ZnO nanoparticles	Pad printing	[31]	2009
P3MHOCT:ZnO nanoparticles	Screen printing	[32]	2009
P3MHOCT:ZnO nanoparticles	Screen printing	[33]	2009
P3HT:PCBM	Spray coating	[28]	2009
P3HT:PCBM	Ink-jet printing	[23]	2010
P3HT:PCBM	Spin coating	[34]	2011
P3HT:PCBM	Gravure printing	[35]	2011
P3HT:PCBM	Spray coating	[10]	2011
P3HT:PCBM	Dip coating	[26]	2012
P3HT:PCBM	Slot die coating	[36]	2012
P3HT:PCBM	Gravure printing	[24]	2012
P3HT:PCBM	Spray coating	[37]	2012
P3HT:PCBM	Spray coating	[27]	2012
POD2T-DTBT:PCBM	Blade coating	[5]	2012
P3HT:bisindene-C60	R2R coating	[38]	2012
PCDTBT:PCBM	Spray coating	[39]	2012
PFB:F8BT	Spray coating	[40]	2014
P3HT:PCBM	Spray coating	[41]	2014
PBDTTT-C-T:PCBM	Blade coating	[42]	2014
PCDTBT:$PC_{71}BM$	Blade coating	[43]	2014

2. Printing methods

Printing is usually been used to describe a method by which a layer of ink is transferred from a stamp to a substrate through a reversing reaction [25]. Fig. 1 contains an illustration of printing apparatus. Printing methods thus include flexographic printing, offset printing, gravure printing, screen printing and ink-jet printing. In the printing method, the

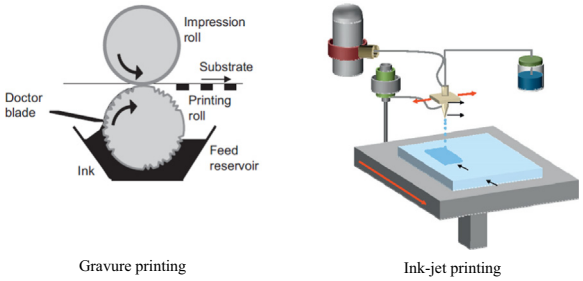

Fig. 1. Illustration of printing apparatus.

choice of the solvents for ink preparation has been identified as an important parameter for active layer surface morphology [24,44,45]. Voigt et al. [24] studied the effect of solvents on the properties of the ink for the gravure printing method. They concluded that in optimizing a solvent for a P3HT:PCBM ink, the boiling point of the solvent must be above 170 °C and the vapor pressure of the solvent should be below 8.8 mmHg. Besides, the solvents also must completely dissolve the P3HT:PCBM to obtain a homogenous film with smooth surface.

The printability of the photoactive and hole transport layer for printing method is an issue that has been focused by many researchers [23,44]. In 2009, Eom et al. [46] demonstrated the roles of additives in ink-jet printed PEDOT:PSS layer in devices efficiency. Glycerol and surfactant, ethylene glycol butyl ether (EGBE), have been used to optimize PEDOT:PSS inks properties. The results showed that PEDOT:PSS film with glycerol 6 wt% and 0.2 wt% EGBE had the best uniform film thickness and density. The PSC fabricated using PEDOT:PSS without any additives showed very poor performance, compared to devices fabricated using PEDOT:PSS with additives. This is due to the improvement of the surface morphology and the improved charge collection by increased conductivity of the PEDOT:PSS with glycerol compared with pure PEDOT:PSS.

In 2010, Eom and his group [23] optimized the inkjet-printing of an active layer by the addition of high b.p. additives such as 1,8 octanedithiol (ODT), o-dichlorobenzene (ODCB), and 1-chloronaphthalene (Cl-naph), to chlorobenzene (CB) solvents. The inkjet-printed solar cells fabricated with inks containing additives have improved crystallinity and better light harvesting properties over a wider spectral region when compared to spin coated devices. The addition of high b.p. additives also reduced the RMS roughness of the film, because these high b.p. additives allow for a controlled evaporation and sufficient time for self-organization to occur. Besides, the additives enhanced the wettability of the P3HT:PCBM inks on the PEDOT:PSS layer, producing an active layer with uniform film morphology and reducing the coffee-ring effect. The overall performance of the inkjet-printed devices with additives is higher than inkjet-printed devices without additives. Jørgensen et al. [32] synthesized thermo-cleavable solvents for application in screen-printed polymer solar cells. This new solvent shows low volatility at ambient conditions, but decomposes thermally at 130–180 °C to low-boiling and high volatile products. Low volatility solvents are needed in printing methods, since the ink is fully exposed to the atmosphere and smeared over a large surface area during printing, speeding the evaporation of solvents with high volatility [32,33].

3. Coating methods

Coating describes a process by which a layer of ink is transferred to the substrate by essentially pouring, painting, spraying, casting or smearing it over the surface [25]. Examples of coating techniques include blade coating, spray coating, painting, slot-die coating, curtain coating and slide coating. Spray coating methods have great potential for large scale production with less or no material wastage, compared to conventional methods such as spin coating methods.

3.1. Blade coating

Blade coating has the advantage of exhibiting large-area uniformity, small amount of material waste, preventing of interlayer dissolution, compatibility to a roll-to-roll fabrication, as well as a more economical use of active material while still giving the possibility to prepare well-defined films [6,17,42]. A rapid drying process in the blade coating method will prevent fabrication throughput from being slowed by the conventional solvent annealing process [42]. In this method, the film thickness can be controlled by adjusting the fabrication parameters such as the solution concentration, the blade gap and the blade coating speed [6]. Fig. 2 illustrates the schematic diagram of the blade coating method. Tsai et al. [42] demonstrated a high performance of PSC based on PBDTTT-C-T:PCBM with the chlorine-free solvents toluene and xylene using blade coating methods. The main reason for the improvement in PSC performance is the good solubility of PBDTTTC-T in the chlorine-free solvents. Also, they observed smoother surfaces in blade coated film compared to spin coated film, which relatively increased the PCE of the blade coated PSC.

The same phenomenon was observed by Chang et al. [6] when they prepared P3HT:PCBM PSC using different coating techniques such as spin coating, blade coating, blade coating on a hot plate, as well as blade and spin coating. The polymer films made by blade coating using chlorine-free solvents toluene were more ordered than those by spin coating because the polymer chains are relatively free to move in the absence of centrifugal force. Thus, they concluded that such methods do not need any post-production treatment, such as solvent annealing and thermal annealing, to produce the desired ordered and interpenetrating morphology in polymer films. Schneider et al. [17] conducted a systematic study on the relevant parameters of the doctor blading process such as preparation atmosphere, coating temperature, evaporation rate, solvents and active layer thickness. They found that like other methods for preparing PSC, this method also leads to exposure to photooxidation when prepared under atmospherics conditions. In terms of coating temperature, 70 °C is considered as the optimum coating temperature, since it will lead to slower solvent evaporation thus forms a thermodynamically more favorable morphology in this system. Somehow, overly decelerated drying is not advantageous for this technique. Overall, it appears that choice of solvent is the most important parameter, since it will affect the

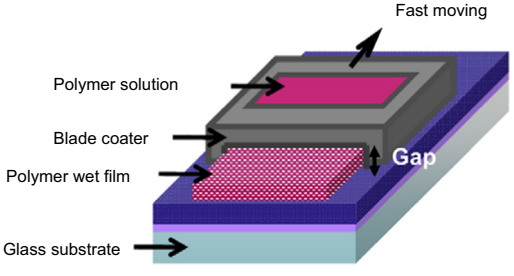

Fig. 2. Schematic diagram of blade coating [6].

evaporation rate, which consequently influences the morphology formation and the performance of the PSC.

3.2. Spray coating

Spray coating is a technique in which the printing ink is forced through a nozzle whereby a fine aerosol will be formed [25]. In a spray coating process, characteristic performance of polymer solar cells is limited by some drawbacks such as isolated droplets, non-uniform surface and pinholes [10,47]. There are few process parameters for the spray coating that has been extensively being studied such as distance between sample and airbrush, flow rate, pressure, substrate temperature, concentration of the blend solution, spray duration, cosolvent mixture and number of times the substrate is sprayed [12,13,48,49]. Table 2 summarizes the previous researches on the spray coating methods with the optimum value for each spray coating process parameters. The highest PCE reported is 4.1% with cell area of 2.5 cm^2 [48]. They used the mixed solvents to prepare the polymer active layer and also heated the substrate to 40 °C. It has been demonstrated that scaling up the cell area leads to decrement in PCE. Park et al. [13] and Kang et al. [27] demonstrated that the PCE of the devices were decreasing with the increment of the cell area. This is due to the high sheet resistance of the transparent electrode and the difficult optimization of large-area thin film deposition [13]. Fig. 3 illustrates the electro-spray coating apparatus and commercially available air-brush spray coating apparatus.

3.2.1. Nozzle to substrate distance

Distance between nozzle and substrate has been identified as one of the process parameters in spray coating that had a great impact on the morphology of deposited layer. Many researches have been conducted to analyze and optimize the nozzle to substrate distance for the deposition of active layer. Vak et al. [53] identified three different regions between airbrush nozzle and substrates, which are “wet”, “intermediate”, and “dry”. They found that the best linear control over thickness as a function of spraying time was in the “intermediate zone”. Susanna et al. [48] observed the same phenomenon in which below 15 cm (distance between sample and airbrush) the deposed material remained wet while over 20 cm from the substrate, produced dry and powdery films. The “intermediate” zone is at 17 cm. At this point the samples showed good uniformity with a maximum PCE of 4.1%. Saitoh et al. [39] found that at 10 cm, an irregular and higher thickness film was formed, uniform thickness was formed at 20 cm distance while less uniformity and thickness were observed at 30 cm (nozzle to substrate distance).

3.2.2. Solvent and mixed solvents effect

Different types of solvents such as chlorobenzene (CB), dichlorobenzene (DCB), trichlorobenzene (TCB), *p*-xylene, toluene and many more have been used by researchers to study the effects of solvent on PSC properties and performance [50,52]. Table 3 lists the properties of typical solvents for active layer in PSC. In spray coating methods, the choice of solvents is really important since it will affect the choice of

Table 2
Previous researches on the spray coating methods.

Active layer	Nozzle to substrate distance (cm)	Pressure (psi)	Substrate *T* (°C)	Cosolvent mixture	Spraying time	Thickness (nm)	Cell area	PCE (%)	Ref
P3HT: PCBM	3	20	RT	DCB	–	380	–	2.8	[28]
P3HT: PCBM	–	43.5	RT	oDCB: 1,35-trimethylbenzene (1:0.5)	–	250	20 mm^2	3.1 2.7	[50]
P3HT: PCBM	5	–	–	p-xylene or CB	–	–	0.11 cm^2	–	[12]
P3HT: PCBM	20	14.5	150	–	20 s	–	9 mm^2	3.0	[51]
P3HT: PCBM	17	12	40	DCB:CB (1:5)	3 sprays of 10 s	270	5 × 5 mm^2	4.1	[48]
P3HT: PCBM	3.5	50	RT	DCB	–	250	0.38 cm^2 4.08 cm^2 9.08 cm^2 12.25 cm^2	3.13 2.64 1.79 1.68	[13]
P3HT: PCBM	–	–	RT	DCB	–	200–300	4 mm^2	1.2	[49]
P3HT: PCBM	10	70	50	CB Additional spray coating: DCB	–	173	–	3.06	[10]
P3HT: PCBM	3.5	–	RT	DCB	0.2 ml/min	180–320	0.36 cm^2 15.25 cm^2	3.17 1.33	[27]
P3HT: PCBM	7	–	RT	CB:DIO	10 μl/min	–	14.5 mm^2	3.08	[37]
P1:PCBM	–	–	RT	DCB	–	100	1 cm^2	3.02	[52]
P3HT: PCBM	10	70	RT	CB Additional spray coating: DCB	–	218	–	2.83	[11]
PCDTBT: PCBM	20	1.16	RT	CF: CB (1:5)	20 s	78–140	5 mm^2	1.08	[39]
P3HT:PPV: PCBM	7	–	RT	–	10 s	–	–	–	[14]

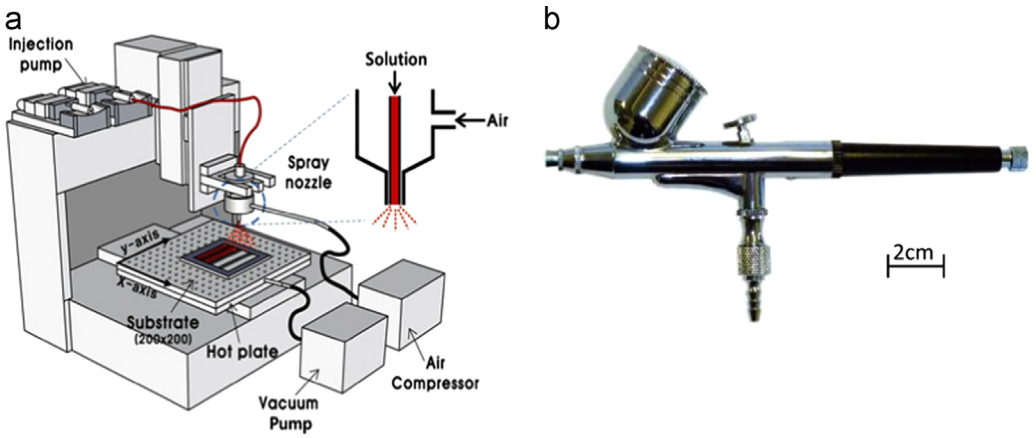

Fig. 3. Schematic diagram of the spray-coating apparatus (a) electro spray coater [27] and (b) air-brush spray coater.

Table 3
Properties of typical solvents for active layer in polymer solar cells.

Solvent	Boiling point (°C)	Vapor pressure at 20 °C (mmHg)	Surface tension (dynes/cm)	Viscosity at 25 °C (mPa)
Chlorobenzene	132	11.8	33.6	0.76
p-xylene	138	9.00	28.4	–
1,2-dichlorobenzene	180	1.20	37.0	1.32
Mesitylene	165	1.86	28.8	1.04
Toluene	110.6	21.9	27.92	–
Chloroform	61.2	–	26.67	0.542

nozzle–substrate distance for thickness optimization and film morphology [52]. Basically, the concept behind choosing a solvent is to choose a fast drying solvent to prevent droplets from re-dissolving sublayers but not so fast so as to allow for a homogenous and pin-hole free film to form [52]. The pin-hole thin films are undesirable in spray coating thin films, because such films will deteriorate the performance of PSC devices. To produce pin-hole free films, the amount of liquid sprayed on the substrate should be greater than a minimal threshold, so that the droplets placed on the substrate can merge into a full wet layer [54]. Besides, by controlling the phase evaporation, by means of substrate heating or mixed solvents, the homogeneity of the thin films is assured.

Hoth et al. [50] performed a systematic study on the surface topography and the morphology of spray coated mono- and bilayers based on pristine solvents compared to mono- and bilayers based on multiple solvents systems. Their findings are that the solvent properties such as boiling point, vapor pressure, viscosity and surface tension have a massive impact on the topography of the spray coated devices. Interestingly, they found that the spray coated devices based on multiple solvents had 10 times higher surface roughness compared to doctor bladed films. This spray coated devices also demonstrated higher PCE (3.1%) compared to doctor bladed films. Thus, this reflects that the large surface roughness of the films does not generally affect the device performance.

Steirer et al. [12] observed notable differences in wetting and film formation from two different types of solvent, chlorobenzene and *p*-xylene, respectively. The improvement in wetting of a single deposited layer from *p*-xylene and the dominant coffee-stained in CB deposited layer were observed and this is related to the lower surface tension of the *p*-xylene solutions. As 50 additional layers plus flood layers were sprayed, the morphology of CB-sprayed film was effectively smoothed while *p*-xylene sprayed film did not have the same effect. The optical micrographs image of P3HT:PCBM active layers prepared from different types of solvents is shown in Fig. 4. It can be clearly seen that active layers prepared from chlorobenzene were significantly smoother and more homogenous than active layers prepared from others solvent [29]. The device parameters for devices prepared from CB and *p*-xylene exhibited similar values; however, the PCE of *p*-xylene is higher than CB but with higher error bars. Thus, Green et al. [29] suggested that CB is the most suitable solvent for a systematic study of devices prepared by airbrush spray deposition.

Chen et al. [55] demonstrated that the incorporation of 2 vol% 1,8-octanedithiol (OT) into the P3HT solution (in CB) enhanced the ordering of the P3HT domains thus improved the PCE from 0.41% to 1.55% without any annealing treatment or device optimization. However, they did not vary the additives contents. Recently, Kim et al. [37] performed a comprehensive study on the effects of solvent additives on the performances of spray coated P3HT:PCBM PSC devices. The optical microscope images (see Fig. 5) of the spray coated P3HT:PCBM films show that the films without DIO formed pancake-shaped blend droplets, while the pancake boundaries gradually disappeared with the increasing of DIO contents and fully

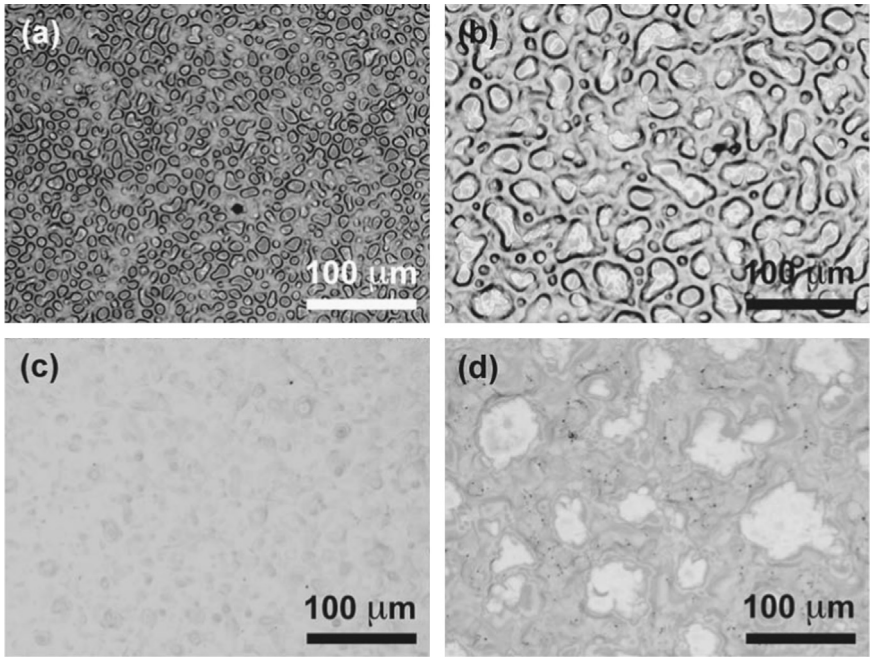

Fig. 4. Optical micrographs of P3HT:PCBM active layers prepared from (a) chloroform, (b) toluene, (c) chlorobenzene, and (d) p-xylene [29].

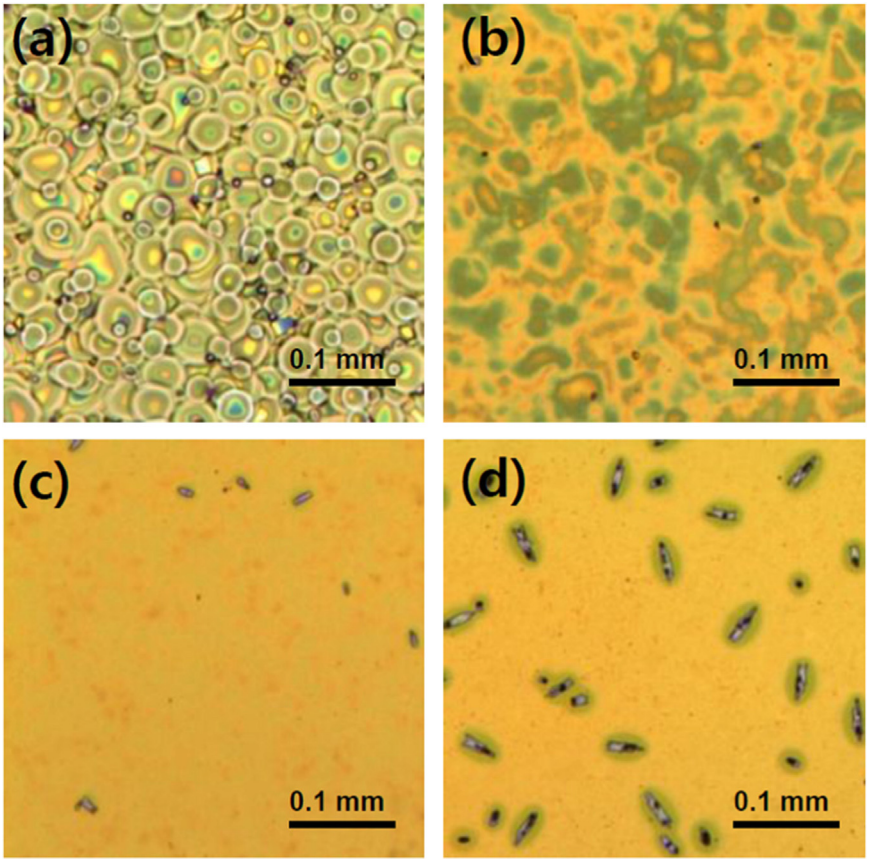

Fig. 5. Optical microscope images (0.1×0.1 mm^2) of the e-sprayed P3HT:PCBM films achieved with various amounts of added DIO: (a) 0 vol%; (b) 3 vol%; (c) 6 vol% and (d) 8 vol% [37].

eliminate at 6 vol%. The rougher surfaces were observed in film without DIO compared to the film with DIO. In terms of performance, the devices fabricated without any additive showed very poor performance with low values of PCE, short circuit current (I_{sc}) and fill factor (FF). This may be related to the morphology of the e-spray coated PSC where there is an interfacial boundary between the droplets in the films that have a tendency to hinder charge transport resulting in increases of the series resistance (R_s).

Lee et al. [10] observed that the active layer prepared using DCB as a solvent produced different surface film compared to film prepared using chlorobenzene and chloroform, which has been attributed to low vapor pressure of DCB. They also applied an additional solvent spray deposition to improve the interconnection among droplets and reduced amounts of pinholes in the spray coated PSC films [10]. They observed that the additional solvent spray process could induce the solvent annealing effect and it also helps in eliminating most of the pinholes. The disappearances of thick edges of the active layer are also possible due to the dissolution of the previously sprayed droplets. Based on Fig. 6, the vibronic shoulder of the additional solvent spray deposition without thermal annealing demonstrates a similar peak to the reference spray coated device without thermal annealing. This proved that the additional solvent coating enhanced the crystallinity of the P3HT chains.

3.2.3. *Substrate temperature and annealing treatment*

Green et al. [29] had performed a comprehensive study on the effect of annealing temperature on the performance of spray coated devices. The devices efficiency is changed with the annealing temperature and this is primarily due to the change in the short circuit current density (I_{sc}). By comparing with the as-deposited devices, a significant enhancement of the fill factor (FF) and I_{sc} was observed for annealing devices most likely due to an improvement of the active layer ordering, which facilitates transport of charge to the contacts. However, at 200 °C annealing, significant deterioration of the device performance can be observed due to extensive phase separation leading to the formation of crystallites of PCBM. Lee et al. [10] observed that morphological surface of the spray coated devices in micrometer scale does not get affected by thermal annealing at 150 °C. However, contradictory results were obtained by Dang et al. [34] where they observed that annealing improved the morphological structure of the spin cast active layers towards better organization and phase separation.

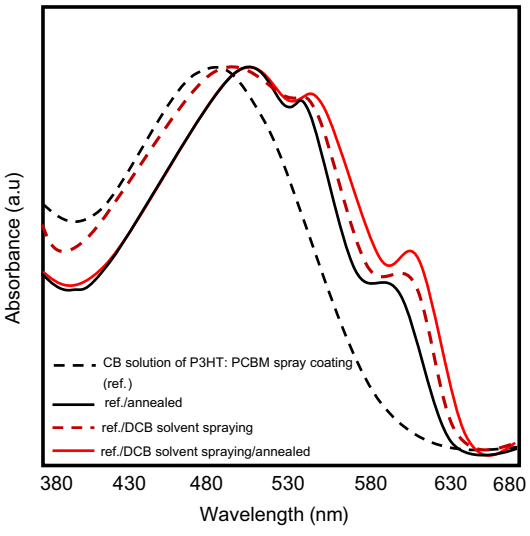

Fig. 6. UV–vis spectra of spray coated PSC with and without annealing [10].

Lee et al. [10] explained in detail on the microscopic change of active layer in the process of additional solvent spraying and thermal annealing as depicted in Fig. 7. As can be seen in Fig. 7(a) and (b), the coffee ring effect effectively binds every droplet tightly so that reorganization of the P3HT:PCBM is not possible and eventually blocks the enhancement upon thermal annealing (Fig. 7 (b)). When additional solvents with low vapor pressure (DCB) were sprayed on the active layer, the solvent entered into the space of previously deposited droplets (Fig. 7(c)), dissolved the dried droplets and the thick boundary, and started to connect to form a larger droplet. Thus, the solvent annealing effect can be obtained in active layer applying additional solvent spray coating process by controlling the total time of spraying and flow rate of sprayed droplets.

Kim et al. [37] obtained a PCE of 2.98% for as-deposited fully e-sprayed PSC, and this value was further increased to 3.08% with the addition of a postannealing treatment. The main reason for the performance enhancement is that the annealing treatment is able to lower R_s of the PSC. Aziz et al. [14] studied the effects of solvent annealing with subsequent thermal annealing on the crystallinity of spray coated ternary blends films prepared using low boiling point solvents. The improvement in crystallinity was observed in solvent annealed and thermal annealed films at 130 °C and 140 °C mainly due to higher ordering in such films. However, at high annealing temperature 150 °C, the crystallinity dropped. They explained this phenomenon based on the weak van der Waals forces formed in organic crystals in these samples. It has been suggested that this weak intermolecular force in P3HT molecules was evolved during high annealing treatment that leads to crystallinity reduction. Besides, the interruption of PCBM and PPV molecules in the ordering of P3HT chain stacking during annealing treatment is also one of the reasons.

Substrate temperature is one of the parameter that can be manipulated in order to optimize the morphology of the spray coated solar cells. In 2011, Susanna et al. [48] studied the effects of substrate temperature on the morphology and performance of mixed solvents spray-coated solar cells. They found that the optimal temperature is 40 °C for DCB:CB systems, as there is a correct balance between the evaporation rates of the two solvents. Girotto et al. [54] explained in detail about the effect of substrate temperature on the PEDOT:PSS thin film formation. At a substrate temperature of 75 °C, which is close to the boiling point of isopropyl alcohol (IPA), coffee ring shapes are visible. This is because the liquid dries immediately upon impact with the substrate and not able to cover the

entire substrate surface. When the substrate temperature is reduced to 55 °C, a strong coffee ring effect is still present due to the contraction that prevents the coverage of the sides of the deposition, along the edges of the sample. The complete wetting of the whole surface is obtained at substrate temperature of 30 °C. They relate this phenomenon with Marangoni flows that produce an advancing velocity of the contact line, which recovers the unwetted area, as shown in Fig. 8.

For fully spray coated devices, depositing a PEDOT:PSS buffer layer or top-electrode from aqueous solution on a non-polar active layer in inverted PSC is commonly considered a very challenging task [27,56]. This is due to the wettability problem of highly hydrophilic PEDOT:PSS aqueous solution into the P3HT:PCBM film, resulting in very poor device performance [15,27]. For fully spray coated inverted devices, a very high RMS roughness, as shown in Fig. 9 for spray coated PEDOT:PSS layer on top of the active layer, was observed by Kang et al. [27] that resulted in decreased device performance compared to spin coated devices. They heated the substrate up to 80 °C to improve wettability so that uniform PEDOT:PSS film on top of active layer can be produced. The PCE of the devices were improved with the increasing of the substrate temperature. They further optimize the thermal annealing process by changing the annealing method from pre-annealing to postannealing and the PCE of the device were further improved from 2.93% to 3.17%. This is due to the enhancement of interface contact at the PEDOT:PSS and active layer.

An interesting phenomenon for the spray coated solar cells under constant illumination from the solar simulator has been observed by Lewis et al. [49] which is called as "photoannealing". Photoannealing of active layer improves morphology and has cured some of the weak points, thus improving I_{sc} and FF. This has been shown in the *I–V* curve where there is a sudden change of *I–V* characteristics after certain amount of time and maximum PCE were achieved after 2.5 h under illumination. Interestingly, the performance improvement under illumination only happened for the sprayed devices, not in the spin coated devices.

Griffin et al. [57] deposited a thin film of molybdenum oxide (MoOx) as the hole extraction layer by ultrasonic spray coating methods. They observed that the efficiency of the devices depends strongly on the annealing temperature used to convert the ammonium molybdate tetrahydrate to MoOx.

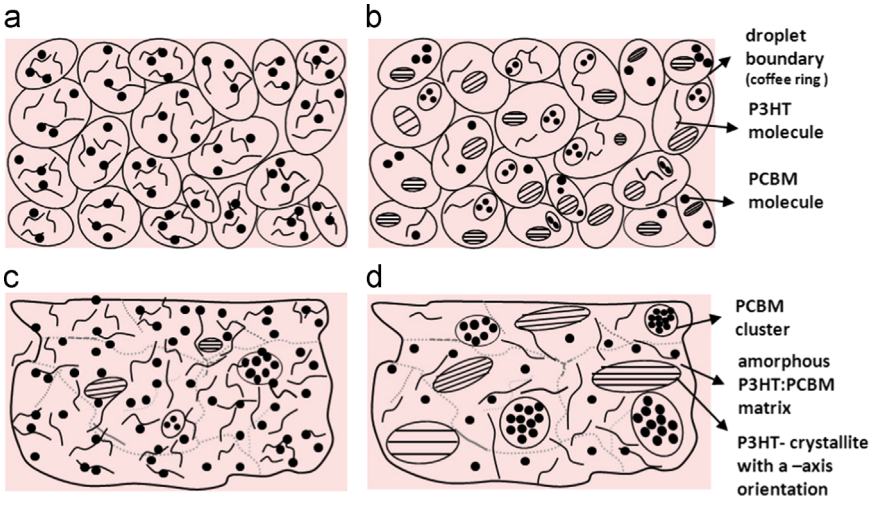

Fig. 7. Schematic diagram of the microscopic change of active layer in the process of additional solvent spraying and thermal annealing (a) CB solution of P3HT:PCBM spray coating (ref.), (b) ref./annealed, (c) ref./DCB solvent spraying and (d) ref./DCB solvent spraying/annealed [10].

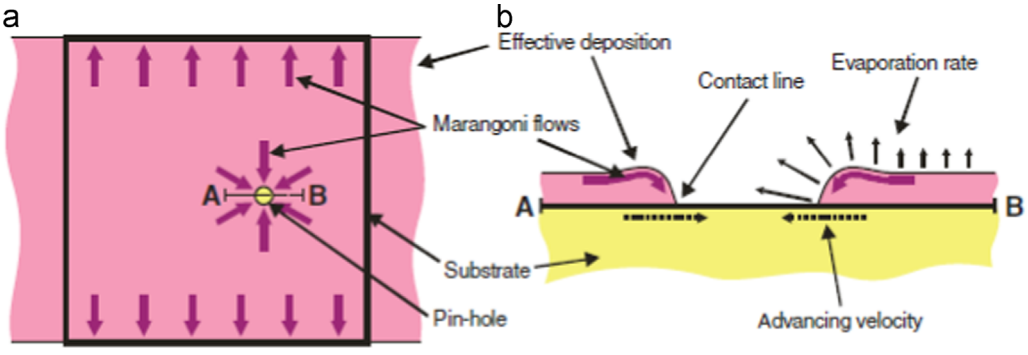

Fig. 8. Schematic of the evolution of the liquid layer during the drying process: (a) top view of the liquid coverage of the substrate and its surroundings, together with the involved Marangoni flows; (b) cross section A–B [54] (reproduced with permission from Advanced Functional Materials 21,1 (2011). Copyright 2011 WILEY-VCH Verlag GmbH & Co. KGaA, Weinheim).

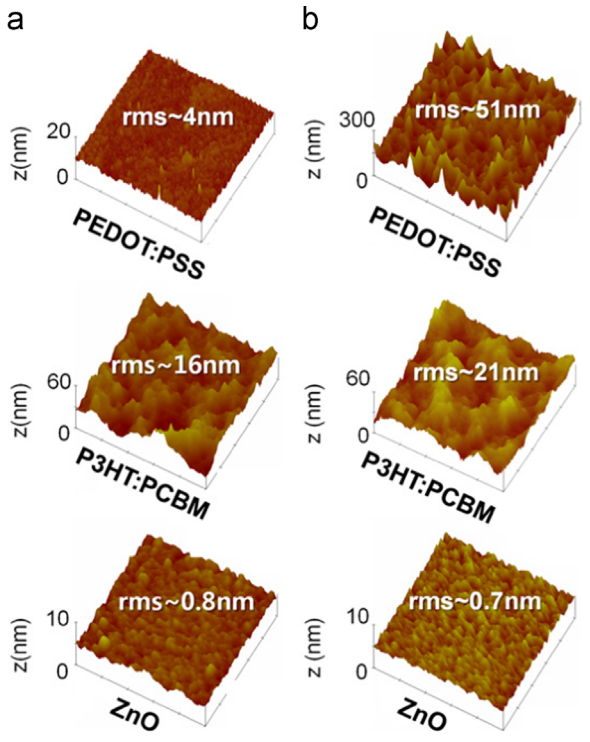

Fig. 9. AFM images and RMS roughness of the three different layers in the inverted organic solar cell coated by (a) spin- and (b) spray coating process. AFM image scans are $5 \times 5\ \mu m^2$ [27].

They suggested that the thermal anneal process removes trapped solvent and ammonium from the film. Therefore, the structural arrangement accompanied with the chemical conversion of the precursor to MoOx occurred during annealing process. Recently, Li and coworkers [58] deposited the silver electrode using spray coating methods. They successfully modified the morphology of spray coated silver electrode by performing hydrochloric acid solvent vapor annealing (SVA) during the fabrication process. High conductivity and high precision of the silver electrode were obtained by incorporating SVA due to the elimination of boundary diffraction effect. The findings of their research are beneficial for further performance improvement of printed electronics and provide a promising method for the preparation of large scale PSC with high precision and low cost, especially for the fabrication of touch screen circuit.

4. Summary

The relevant parameters in spray coating processes have been reviewed. Spray coating methods appear attractive for large scale production of PSC. This method has no-limitation in substrate size and low utilization of polymers which is promising to substitute the conventional spin coating methods. Nozzle to substrate distance, solvent and mixed solvent effects, substrate temperature, and annealing treatment have been identified as the relevant parameters in spray coating processes. By setting the right distance between nozzle and substrate, wet, intermediate, and dry films may be produced. Solvent selection and additives appear to have major impacts on the morphological properties of the spray coated thin films. The substrate temperature parameter can also be manipulated in order to optimize the morphology of the deposited layers. Finally, annealing treatment has also been proven to be a successful method to modify the morphology and improve the performance of spray coated PSC.

Acknowledgments

The authors acknowledge the financial support by the Ministry of Education (MOE) Malaysia under Grant no. Q.J130000.3009.00M02.

References

[1] Z. Hu, J. Zhang, S. Xiong, Y. Zhao, Sol. Energy Mater. Sol. Cells 99 (2012) 221–225.
[2] P. Schilinsky, C. Waldauf, C.J. Brabec, Adv. Funct. Mater. 16 (13) (2006) 1669–1672.
[3] A. Abdellah, B. Fabel, P. Lugli, G. Scarpa, Org. Electron.: Phys. Mater. Appl. 11 (6) (2010) 1031–1038.
[4] C.J. Brabec, N.S. Sariciftci, J.C. Hummelen, Adv. Funct. Mater. 11 (1) (2001) 15–26.
[5] S.-L. Lim, E.-C. Chen, C.-Y. Chen, K.-H. Ong, Z.-K. Chen, H.-F. Meng, Sol. Energy Mater. Sol. Cells 107 (2012) 292–297.
[6] Y.-H. Chang, S.-R. Tseng, C.-Y. Chen, H.-F. Meng, E.-C. Chen, S.-F. Horng, C.-S. Hsu, Org. Electron. 10 (5) (2009) 741–746.
[7] S.K. Jang, S.C. Gong, H.J. Chang, Synth. Met. 162 (5–6) (2012) 426–430.
[8] H. Wang, Y. Zheng, L. Zhang, J. Yu, Sol. Energy Mater. Sol. Cells 128 (2014) 215–220.
[9] I. Hwang, C.R. McNeill, N.C. Greenham, Synth. Met. 189 (2014) 63–68.
[10] J.-H. Lee, T. Sagawa, S. Yoshikawa, Org. Electron. 12 (12) (2011) 2165–2173.
[11] J.-H. Lee, T. Sagawa, S. Yoshikawa, Thin Solid Films 529 (2013) 464–469.
[12] K.X. Steirer, M.O. Reese, B.L. Rupert, N. Kopidakis, D.C. Olson, R.T. Collins, D.S. Ginley, Sol. Energy Mater. Sol. Cells 93 (4) (2009) 447–453.
[13] S.-Y. Park, Y.-J. Kang, S. Lee, D.-G. Kim, J.-K. Kim, J.H. Kim, J.-W. Kang, Sol. Energy Mater. Sol. Cells 95 (3) (2011) 852–855.
[14] F. Aziz, A.F. Ismail, M. Aziz, T. Soga, Chem. Eng. Process.: Process Intensif. 79 (2014) 48–55.
[15] P. Kumar, K. Santhakumar, J. Tatsugi, P.K. Shin, S. Ochiai, Jpn. J. Appl. Phys. 53 (1S) (2014) 1–8.
[16] S.E. Shaheen, R. Radspinner, N. Peyghambarian, G.E. Jabbour, Appl. Phys. Lett. 79 (18) (2001) 2996–2998.
[17] A. Schneider, N. Traut, M. Hamburger, Sol. Energy Mater. Sol. Cells 126 (0) (2014) 149–154.
[18] S.I. Na, D.W. Park, S.S. Kim, S.Y. Yang, K. Lee, M.H. Lee, Semicond. Sci. Technol. 27 (12) (2012) 1–5.
[19] C. Yang, E. Zhou, S. Miyanishi, K. Hashimoto, K. Tajima, ACS Appl. Mater. Interfaces 3 (10) (2011) 4053–4058.
[20] Y. Sun, Y. Zhang, Q. Liang, Y. Zhang, H. Chi, Y. Shi, D. Fang, RSC Adv. 3 (30) (2013) 11925–11934.
[21] L. Blankenburg, K. Schultheis, H. Schache, S. Sensfuss, M. Schrödner, Sol. Energy Mater. Sol. Cells 93 (4) (2009) 476–483.
[22] J.-A. Jeong, J. Lee, H. Kim, H.-K. Kim, S.-I. Na, Sol. Energy Mater. Sol. Cells 94 (10) (2010) 1840–1844.
[23] S.H. Eom, H. Park, S.H. Mujawar, S.C. Yoon, S.-S. Kim, S.-I. Na, S.-J. Kang, D. Khim, D.-Y. Kim, S.-H. Lee, Org. Electron. 11 (9) (2010) 1516–1522.
[24] M.M. Voigt, R.C.I. Mackenzie, S.P. King, C.P. Yau, P. Atienzar, J. Dane, P. E. Keivanidis, I. Zadrazil, D.D.C. Bradley, J. Nelson, Sol. Energy Mater. Sol. Cells 105 (2012) 77–85.
[25] F.C. Krebs, Sol. Energy Mater. Sol. Cells 93 (4) (2009) 394–412.
[26] Z. Hu, J. Zhang, S. Xiong, Y. Zhao, Org. Electron. 13 (1) (2012) 142–146.
[27] J.-W. Kang, Y.-J. Kang, S. Jung, M. Song, D.-G. Kim, C. Su Kim, S.H. Kim, Sol. Energy Mater. Sol. Cells 103 (2012) 76–79.
[28] C. Girotto, B.P. Rand, J. Genoe, P. Heremans, Sol. Energy Mater. Sol. Cells 93 (4) (2009) 454–458.

[29] R. Green, A. Morfa, A.J. Ferguson, N. Kopidakis, G. Rumbles, S.E. Shaheen, Appl. Phys. Lett. 92 (3) (2008) 033301–033303.
[30] K. Thomas, H. Hans-Heinrich, N. Dieter, Chem. Mater. 17 (2005) 6532–6537.
[31] F.C. Krebs, Sol. Energy Mater. Sol. Cells 93 (4) (2009) 484–490.
[32] M. Jørgensen, O. Hagemann, J. Alstrup, F.C. Krebs, Sol. Energy Mater. Sol. Cells 93 (4) (2009) 413–421.
[33] F.C. Krebs, M. Jørgensen, K. Norrman, O. Hagemann, J. Alstrup, T.D. Nielsen, J. Fyenbo, K. Larsen, J. Kristensen, Sol. Energy Mater. Sol. Cells 93 (4) (2009) 422–441.
[34] M.T. Dang, G. Wantz, H. Bejbouji, M. Urien, O.J. Dautel, L. Vignau, L. Hirsch, Sol. Energy Mater. Sol. Cells 95 (12) (2011) 3408–3418.
[35] M.M. Voigt, R.C.I. Mackenzie, C.P. Yau, P. Atienzar, J. Dane, P.E. Keivanidis, D.D.C. Bradley, J. Nelson, Sol. Energy Mater. Sol. Cells 95 (2) (2011) 731–734.
[36] S.R. Dupont, M. Oliver, F.C. Krebs, R.H. Dauskardt, Sol. Energy Mater. Sol. Cells 97 (2012) 171–175.
[37] Y. Kim, G. Kim, J. Lee, K. Lee, Sol. Energy Mater. Sol. Cells 105 (2012) 272–279.
[38] M. Schrödner, S. Sensfuss, H. Schache, K. Schultheis, T. Welzel, K. Heinemann, R. Milker, J. Marten, L. Blankenburg, Sol. Energy Mater. Sol. Cells 107 (2012) 283–291.
[39] L. Saitoh, R.R. Babu, S. Kannappan, K. Kojima, T. Mizutani, S. Ochiai, Thin Solid Films 520 (7) (2012) 3111–3117.
[40] M. Noebels, R.E. Cross, D.A. Evans, C.E. Finlayson, J. Mater. Sci. 49 (12) (2014) 4279–4287.
[41] Y. Zheng, S. Li, X. Yu, D. Zheng, J. Yu, RSC Adv. 4 (32) (2014) 16464–16471.
[42] P.T. Tsai, C.Y. Tsai, C.M. Wang, Y.F. Chang, H.F. Meng, Z.K. Chen, H.W. Lin, H.W. Zan, S.F. Horng, Y.C. Lai, P. Yu, Org. Electron.: Phys. Mater. Appl. 15 (4) (2014) 893–903.
[43] S. Alem, J. Lu, R. Movileanu, T. Kololuoma, A. Dadvand, Y. Tao, Org. Electron. 15 (5) (2014) 1035–1042.
[44] P. Kopola, T. Aernouts, S. Guillerez, H. Jin, M. Tuomikoski, A. Maaninen, J. Hast, Sol. Energy Mater. Sol. Cells 94 (10) (2010) 1673–1680.
[45] C.N. Hoth, S.A. Choulis, P. Schilinsky, C.J. Brabec, Adv. Mater. 19 (22) (2007) 3973–3978.
[46] S.H. Eom, S. Senthilarasu, P. Uthirakumar, S.C. Yoon, J. Lim, C. Lee, H.S. Lim, J. Lee, S.-H. Lee, Org. Electron. 10 (3) (2009) 536–542.
[47] S. Colella, M. Mazzeo, G. Melcarne, S. Carallo, G. Ciccarella, G. Gigli, Appl. Phys. Lett. 102 (20) (2013) 203307.
[48] G. Susanna, L. Salamandra, T.M. Brown, A. Di Carlo, F. Brunetti, A. Reale, Sol. Energy Mater. Sol. Cells 95 (7) (2011) 1775–1778.
[49] J.E. Lewis, E. Lafalce, P. Toglia, X. Jiang, Sol. Energy Mater. Sol. Cells 95 (10) (2011) 2816–2822.
[50] C.N. Hoth, R. Steim, P. Schilinsky, S.A. Choulis, S.F. Tedde, O. Hayden, C.J. Brabec, Org. Electron. 10 (4) (2009) 587–593.
[51] K.-J. Kim, Y.-S. Kim, W.-S. Kang, B.-H. Kang, S.-H. Yeom, D.-E. Kim, J.-H. Kim, S.-W. Kang, Sol. Energy Mater. Sol. Cells 94 (7) (2010) 1303–1306.
[52] W. Nie, R. Coffin, J. Liu, C.M. MacNeill, Y. Li, R.E. Noftle, D.L. Carroll, Int. J. Photoenergy 2012 (2012) 7.
[53] D. Vak, S.-S. Kim, J. Jo, S.-H. Oh, S.-I. Na, J. Kim, D.-Y. Kim, Appl. Phys. Lett. 91 (8) (2007) 081102–081103.
[54] C. Girotto, D. Moia, B.P. Rand, P. Heremans, Adv. Funct. Mater. 21 (1) (2011) 64–72.
[55] L.-M. Chen, Z. Hong, W.L. Kwan, C.-H. Lu, Y.-F. Lai, B. Lei, C.-P. Liu, Y. Yang, ACS Nano 4 (8) (2010) 4744–4752.
[56] A. Colsmann, M. Reinhard, T.-H. Kwon, C. Kayser, F. Nickel, J. Czolk, U. Lemmer, N. Clark, J. Jasieniak, A.B. Holmes, D. Jones, Sol. Energy Mater. Sol. Cells 98 (2012) 118–123.
[57] J. Griffin, A.J. Pearson, N.W. Scarratt, T. Wang, D.G. Lidzey, A.R. Buckley, Org. Electron. 15 (3) (2014) 692–700.
[58] S.G. Li, Y.F. Zheng, J. Cheng, M.J. Tu, J.S. Yu, J. Mater. Sci.—Mater. Electron. 25 (2014) 5013–5019.